

Field Theoretic Study of Bilayer Membrane Fusion: II. Mechanism of a Stalk-Hole Complex

K. Katsov,* M. Müller,[†] and M. Schick[‡]

*Materials Research Laboratory, University of California, Santa Barbara, California; [†]Institut für Theoretische Physik, Göttingen, Germany; and [‡]Department of Physics, University of Washington, Seattle, Washington

ABSTRACT We use self-consistent field theory to determine structural and energetic properties of intermediates and transition states involved in bilayer membrane fusion. In particular, we extend our original calculations from those of the standard hemifusion mechanism, which was studied in detail in the first article of this series, to consider a possible alternative to it. This mechanism involves non-axial stalk expansion, in contrast to the axially symmetric evolution postulated in the classical mechanism. Elongation of the initial stalk facilitates the nucleation of holes and leads to destabilization of the fusing membranes via the formation of a stalk-hole complex. We study properties of this complex in detail, and show how transient leakage during fusion, previously predicted and recently observed in experiment, should vary with lipid architecture and tension. We also show that the barrier to fusion in the alternative mechanism is lower than that of the standard mechanism by a few $k_B T$ over most of the relevant region of system parameters, so that this alternative mechanism is a viable alternative to the standard pathway. We emphasize that any mechanism, such as this alternative one, which affects, even modestly, the line tension of a hole in a membrane, affects greatly the ability of that membrane to undergo fusion.

INTRODUCTION

The fusion of biological membranes is of great importance as it plays a central role *inter alia* in intracellular trafficking, exocytosis, and viral infection (1–6). Given this importance, it might be thought that its mechanism would be well understood, but in fact, it is not. Perhaps the reason for this is that there is an apparent dilemma at the heart of the fusion process. The vesicles or bilayers to be fused must be sufficiently stable with respect to irreversible rupture, to carry out their functions on a reasonably long timescale. It follows that it must be quite energetically expensive to create a large, super-critical, hole in such a membrane. In other words, the free energy barrier to do so must be very large compared to the thermal fluctuation energy $k_B T$. As a consequence, almost all holes created by thermal fluctuations do not have sufficient energy to traverse this barrier, hence they simply shrink and reseal. However, it is inevitable that for fusion to occur, a long-lived hole must be created at some stage of the fusion pathway. The dilemma is that a bilayer can both be stable with respect to rupture and yet readily undergo fusion.

Some of the solution of this puzzle is in place. It is believed that fusion proteins locally expend energy to dehydrate both bilayers to bring them in close proximity. This increases the free energy per unit area of the system, *i.e.*, puts the system under local stress. As a consequence, it is free-energetically favorable for the system to undergo a transformation that results in a decrease of bilayer area. In principle, this can be accomplished both by fusion and/or rupture, but the proteins apparently catalyze the fusion process exclusively.

The standard hemifusion mechanism, proposed 20 years ago by Kozlov and Markin (7), assumes that thermal fluctuations permit the tails of lipids of the *cis* leaves, those of the apposing membranes which are closest to one another, to flip over and form an axially symmetric defect in the dehydrated region, denoted a stalk (8). Due to the tension, the newly joined *cis* layers recede so that the stalk expands radially preserving the axial symmetry, and transforms into a hemifusion diaphragm—a single bilayer consisting of the two remaining *trans* leaves. Only this single bilayer needs to be punctured by a hole in order that a fusion pore be formed and the fusion process be completed. This radial stalk expansion hypothesis, being in qualitative agreement with many experimental observations, was essentially the only model of the fusion process until recently.

In contrast to the hemifusion hypothesis, Monte Carlo simulations of bilayer fusion (9) showed that fusion can evolve through an alternative mechanism (10,11), in which the stalk does not expand radially, but rather elongates in a wormlike fashion. To distinguish the original axially symmetric stalk from the elongated structure, we will call the former the classical stalk for the remainder of the article. Moreover, it was observed that the elongated stalk destabilizes the fusing membranes by greatly enhancing the rate of hole formation in its vicinity. Once such a hole is formed in one bilayer close to the elongated stalk, the stalk encircles it completely, forming a hemifusion diaphragm consisting of the other, as yet intact, bilayer. Subsequent hole formation in this diaphragm completes the fusion process. In a slightly different variant of this scenario, holes form in both bilayers near the stalk before the stalk has completely surrounded the first hole. Fusion is completed when the stalk surrounds both holes. This mechanism was also seen in recent molecular

Submitted July 20, 2005, and accepted for publication October 12, 2005.

Address reprint requests to M. Schick, Tel.: 206-543-9948; E-mail: schick@phys.washington.edu.

© 2006 by the Biophysical Society

0006-3495/06/02/915/12 \$2.00

doi: 10.1529/biophysj.105.071092

dynamics simulations (12,13). It was argued (9) that the stalk lowers the free energy barrier to hole formation by decreasing the effective line tension in that part of the hole in contact with the stalk.

We shall denote the elongated stalk partially surrounding a hole as a stalk-hole complex. As we note below, this stalk-hole complex can decay, i.e., evolve without further free energy cost, into a final fusion pore, so that this complex represents a potential transition state in the fusion process.

A direct consequence of this alternative mechanism is that there can be transient leakage during fusion. Even though leakage is sometimes observed during fusion experiments, it is usually attributed to the presence of fusion proteins which are known, for example, to initiate erythrocyte hemolysis (14). However, the new mechanism predicts that transient leakage stems from the fusion pathway itself and should be observable even during fusion of model membranes in the absence of fusion proteins. Leakage during fusion in such systems has indeed been observed experimentally (15–17). In addition, it is predicted that this transient leakage should be correlated in space and time with fusion. Just such correlated leakage and fusion were recently observed experimentally by Frolov et al. (18). Fusion without detectable leakage is also observed, however (19–21). We shall argue below that the seeming irregularity of leakage accompanying fusion can be explained by the new mechanism. In particular, the extent of this transient leakage depends both on the architecture of the amphiphiles as well as the tension (stress) imposed on the membranes. By decreasing the spontaneous curvature of the amphiphiles and/or reducing the membrane tension, the leakage can be substantially reduced and even completely eliminated in some cases.

A second consequence of the alternative mechanism concerns the transfer of lipids during fusion. In the standard mechanism, the hemifusion diaphragm formed during the fusion process consists of the two *trans* leaves of the fusing bilayers. The two *cis* leaves are joined, permitting the transfer of lipids from an extensive region of the *cis* leaf of one bilayer to the *cis* leaf of the other. Such transfer of lipids has been observed (22,23). In the new, alternative, mechanism a hemifusion diaphragm can also form, but it consists of the *cis* and *trans* leaves of one of the original bilayers. Outside of the hemifusion diaphragm itself, the *cis* layers are joined as in the standard mechanism, again providing the possibility of transfer of lipids from an extensive region of one *cis* leaf to the other. At the circumference of the hemifusion diaphragm itself, there is also contact between the *cis* leaf of one bilayer with the *trans* leaf of the other. Thus, we would expect that the transfer of lipids between them is to be observed in addition to the transfer between *cis* leaves. It has not. We note, however, that whereas the joining of the *cis* leaves is long-lived, and therefore allows the exchange of a macroscopic amount of lipids, the exchange of lipids between the *cis* and *trans* leaves occurs via transient structures and is

microscopic. It is correlated in space and time with the fusion process in a manner similar to the leakage described above. Thus in an experiment that leads to the formation of a fusion pore, such exchange is expected to be much smaller than that between *cis* leaves. Even in an experiment in which the fusion process does not continue to completion, but is halted at the formation of the hemifusion diaphragm, we still expect that lipid exchange between *cis* and *trans* leaves will be much reduced in comparison to exchange between *cis* leaves. This follows from the observation that, in contrast to the extensive amount of area acting as a source for the exchange of lipids between *cis* leaves, in the new mechanism only a limited region, that enclosed by the hemifusion diaphragm, can act as a source of lipids to be transferred from a *cis* to a *trans* leaf.

To clarify the differences between the two mechanisms, and to determine whether one of them is clearly free-energetically favored over the other, we began a program to compare, within the same system, the free energy barriers encountered along each of the two pathways. In a previous article (24), we employed self-consistent field theory (SCFT) to evaluate these barriers assuming that fusion took place via the standard, radially expanding stalk and hemifusion mechanism. The system considered consisted of bilayers of *AB* block copolymer, with fraction f of the *A* monomer, in a solvent of *A* homopolymer. All polymers were characterized by the same polymerization index, and radius of gyration R_g . Comparison of various properties of this specific simulation model of block copolymer amphiphiles with those of membranes consisting of biological lipids permitted an estimate that free energies of a structure in the copolymer simulations were 2.5 times smaller than those of the corresponding structure in the biological system. We calculated the barrier to stalk formation in polymeric bilayers, and from it estimated that in membranes made of biological lipids, this barrier would not exceed $13 k_B T$. The larger barrier in the standard process is that associated with the radial expansion of the hemifusion diaphragm (25), and we estimated this to be in the range of 25–63 $k_B T$, depending upon the lipid architecture and membrane tension. Perhaps one of the most interesting results of this study was the following: the range of variation in amphiphile architecture over which successful fusion can occur is severely restricted by the fact that the fusion process begins with the formation of a metastable, classical stalk. If f is too large, corresponding to lipids with very small spontaneous curvature, stalks between bilayers are never metastable. On the other hand, if f is too small, corresponding to lipids with larger negative spontaneous curvatures, linear (or elongated) stalks became favorable, which destabilize the bilayers completely by causing a transition to an inverted hexagonal phase. Thus, for fusion to occur, the lipid composition of membranes must be tightly regulated. This conclusion also applies to fusion which proceeds via the new mechanism as it, too, begins with the formation of the classical stalk.

In this article, we apply SCFT methods to calculate the fusion barriers in this new, alternative, mechanism. We begin in the first section by calculating the free energy of an isolated hole in a single bilayer as a function of its radius, R , for bilayers under various tensions, γ , and consisting of diblocks of different architectural parameters, f . The result is that, as expected, it is very expensive to create a hole in an isolated bilayer. In the next section, we turn to the calculation of the free energy of the stalk-hole complex. Because this complex is not axially symmetric, our task is much more difficult than our previous calculation of the barriers in the old hemifusion mechanism in which the intermediates were postulated to be axially symmetric. We accomplish our goal by constructing the nonaxially symmetric intermediates from fragments of other excitations which do possess this symmetry, and therefore are more easily obtained. We compare our results for the free energy barrier in the two mechanisms and show that the barrier in the new one is indeed lower than that in the old, although the difference in most of the region of parameters in which fusion can occur successfully is not more than a few $k_B T$. Finally, in the Discussion, we discuss further the reason why the new mechanism is a favorable one. We trace it not only to the reduction of the line tension of a hole when nucleated next to a stalk, but also to the relatively low cost for the stalk to extend linearly. Consequently when a hole appears in the bilayer, a large fraction of its circumference can have its line tension reduced by the nearby presence of a stalk. We conclude with some comments on the dependence of the rate of hole formation in a bilayer on the line tension of the hole. We show that even modest changes in the effective line tension of a hole due to the presence of the elongated stalk in the stalk-hole complex can strongly affect the rate of hole formation, and hence the rate of fusion. Such small changes in line tension, therefore, destabilize what were very stable bilayers and enable them to undergo fusion.

FREE ENERGY OF A HOLE IN AN ISOLATED BILAYER

In this section we discuss the free energy of a circular hole in an isolated bilayer to show that the energy associated with formation of such a defect is high, as is expected if isolated bilayers are stable. Such holes have recently been studied by simulation methods (26–30). The SCFT calculation follows the lines described in our previous article (24). It is straightforward within the SCFT to obtain the free energy, $\Omega_m(T, \Delta\mu, V, A)$, of a bilayer of area A at a temperature T and a difference, $\Delta\mu = \mu_a - \mu_s$, of the bulk chemical potentials of the amphiphile and of the solvent. There is only one independent chemical potential as the system is assumed to be incompressible. The volume of the system is V . Similarly, we denote the free energy of the system without the bilayer, i.e., a homogeneous amphiphile solution, $\Omega_0(T, \Delta\mu, V)$. The difference between these two free energies, in the thermo-

dynamic limit of infinite volume, defines the excess free energy of the bilayer membrane:

$$\delta\Omega_m(T, \Delta\mu, A) \equiv \lim_{V \rightarrow \infty} [\Omega_m(T, \Delta\mu, V, A) - \Omega_0(T, \Delta\mu, V)]. \quad (1)$$

The excess free energy per unit area, in the thermodynamic limit of infinite area, defines the lateral membrane tension

$$\gamma(T, \Delta\mu) \equiv \lim_{A \rightarrow \infty} [\delta\Omega_m(T, \Delta\mu, A)/A]. \quad (2)$$

Changes in this tension γ can be related to changes in the temperature and chemical potential by means of the Gibbs-Duhem equation

$$d\gamma(T, \Delta\mu) = -\delta s dT - \delta\sigma_a d(\Delta\mu), \quad (3)$$

where δs is the excess entropy per unit area, and $\delta\sigma_a$ is the excess number of amphiphilic molecules per unit area. This relation shows that the chemical potential difference, $\Delta\mu$, can be used to adjust the bilayer tension γ .

As discussed previously (24), it is also possible to introduce axially symmetric defects of a specified radius R into the bilayer and to obtain the excess free energy of such structures. The choice of model parameters was dictated by our original Monte Carlo simulations (9) and the details can be found in the first article of this series (24).

Fig. 1 shows the density distribution of hydrophobic (B) and hydrophilic (A) segments in a bilayer with holes of different radii, which are defined as the radial distance in the plane of symmetry to the A/B interface, the point at which the volume fractions of A and B monomers are equal. We find that qualitative features of this profile are not very sensitive to the architectural parameter f or tension γ . The rim of the hole has a shape of a bulb which is typical whenever a flat bilayer has an edge (31–33).

The free energy of such a hole in a bilayer is shown in Fig. 2 *a* as a function of its radius for a bilayer at zero tension and composed of amphiphiles of different architectural parameters, f . One sees that under zero tension the free energy increases essentially linearly with R and the excess free energy of the hole can be written as $2\pi\lambda_H(T, \Delta\mu, R)R$, where λ_H is an effective line tension. As one would expect, this line tension quickly asymptotes to a constant value $\lambda_H(T, \Delta\mu)$ for sufficiently large R . For the bilayer under zero tension composed of amphiphiles with $f = 0.35$, we find $\lambda_H R_g/k_B T = 2.63$. To compare with analogous values for lipid membranes, we convert this to the dimensionless ratio $\lambda_H/\gamma_0 d$, where γ_0 is the free energy per unit area of an interface between coexisting phases of bulk homopolymer A and bulk homopolymer B , and d is the thickness of the bilayer. From our previous work (9), we obtain $\gamma_0 d^2/k_B T = 65.3$, and $d/R_g = 4.47$ so that $\lambda_H/\gamma_0 d = 0.18$. The analogous quantity can be calculated for membranes taking $\lambda_m = 2.6 \times 10^{-6}$ dynes (34, 35), $d_m = 35.9 \times 10^{-8}$ cm (36), and an oil-water tension of $\gamma_m = 50$ dynes/cm, from which $\lambda_m/\gamma_m d_m = 0.14$. Thus the line tensions we obtain are reasonable.

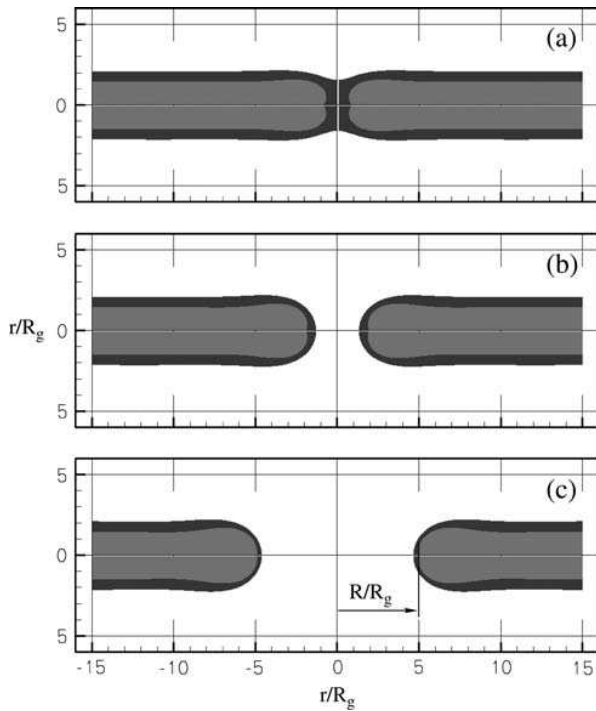


FIGURE 1 Density profiles of bilayers pierced by an isolated hole are shown for three different hole radii: $R/R_g = 1, 2,$ and 5 , with R_g the radius of gyration of all polymers. Only the majority component is shown at each point. Solvent segments are white. Hydrophilic and hydrophobic segments of the amphiphile are shaded dark and light, respectively. The tension is zero and $f = 0.33$.

In Fig. 2 *b* we show the effect of membrane tension on the dependence of the hole free energy on radius R . One sees, as expected, that the free energy of the hole eventually decreases due to the elimination of stressed membrane area. For sufficiently large R , one expects the free energy of the hole to be of the form

$$F_H(R) = 2\pi\lambda_H R - \pi\gamma R^2, \quad (4)$$

with γ the imposed membrane tension. We verified that this form is certainly adequate at large R . At smaller radii, which will be of interest to us, the coefficients λ_H and γ are, themselves, functions of R .

In equilibrium any finite tension will give rise to an eventual membrane rupture. However, for the parameters used in our calculations, the nucleation barrier for the formation of the critical hole is much larger than our estimate for the fusion barrier. Specifically one sees from Fig. 2 *b* that over a wide range of tensions, the maximum value of $F_H(R)$ is no less than $\sim 16 k_B T$. We find no signature of any other barrier along the pathway to rupture, hence this maximum in $F_H(R)$ is the free energy required to form a hole of critical size leading to irreversible membrane rupture. Given our estimate that in systems composed of lipids the free energy is a factor of 2.5 larger than in our system of copolymers, it follows that this barrier to rupture in the former would be of

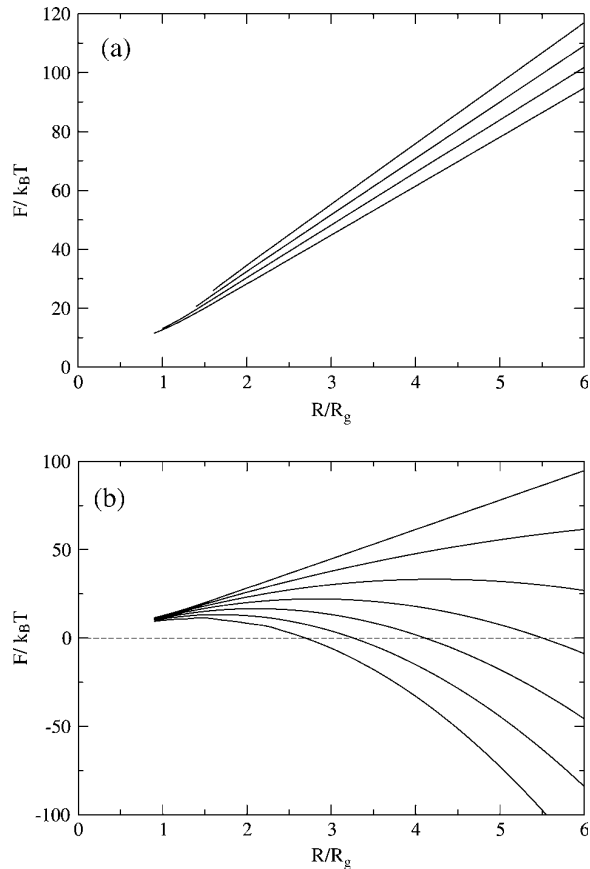


FIGURE 2 (a) Free energy of a hole in an isolated bilayer as a function of R/R_g at zero tension for various amphiphile architectures, f . From top to bottom the values of f are $0.29, 0.31, 0.33,$ and 0.35 . (b) Same as above, but at fixed $f = 0.35$ and various tensions γ/γ_0 . From top to bottom, γ/γ_0 varies from 0.0 to 0.6 in increments of 0.1 .

the order of $40 k_B T$. Thus, as stated, isolated bilayers are very robust against rupture caused by thermal excitation, and it is precisely this stability that makes fusion difficult to understand.

We now turn to the calculation of the stalk-hole complex, which is a possible fusion intermediate. We will show that the barrier to fusion is much less than the barrier to create a hole in each of the two fusing bilayers in the absence of an elongated stalk.

FREE ENERGY OF THE STALK-HOLE COMPLEX

We consider the system of two apposed bilayers. Experimentally it is known that, for fusion of lipid bilayers in aqueous solution to occur, enough water must be removed from the fusion zone so that the *cis* leaves can approach one another to a distance on the order of 1.5 nm (37), approximately one-half the thickness of a single leaf. Bilayers in our calculation are separated by $\sim 1 R_g$, which is again

approximately one-half of the single leaf thickness. Presumably, a smaller distance will reduce the free energy cost of stalk formation, bringing about the formation of more stalks, therefore enlarging the number of sites at which fusion could be initiated, and consequently increasing the rate of fusion. Our concern here, however, is to determine the barrier to fusion in the new mechanism, as opposed to the rate, and compare it to that of the standard hemifusion mechanism under the identical conditions. In the following, we study extensively the effects of the amphiphile architecture and the membrane tension on the barriers. A quantitative study of the effects of hydration is a topic for further investigation.

Immediately before formation of stalk-hole complex

Right after the formation of the initial (classical circular) stalk and just before the formation of the stalk-hole complex, the stalk elongates in a wormlike fashion. For the sake of simplicity, we assume that, in the $z = 0$ (symmetry) plane, this elongated structure has a shape of a circular arc with a fractional angle, $0 \leq \alpha \leq \pi$, and radius R , as shown schematically in Fig. 3. With this choice of the parameters, $\alpha = 0$ corresponds to the classical stalk structure, whereas for $\alpha = \pi$ there is a family of structures that are reminiscent of the inverted micellar intermediate (IMI), studied previously by Siegel (38). In contrast to the IMIs he considered, which were to compete with the formation of a stalk, the structures we consider result from the formation of the stalk and its subsequent wanderings. We assign the same label to our structure as that chosen by Siegel only because of the topological similarity between our structures and his. A density profile of one such structure is shown in Fig. 4. Its radius R is defined as the radial distance to the furthest point on the $z = 0$ plane at which the densities of hydrophobic and hydrophilic segments are equal, and is shown in the figure. We denote its free energy $F_{\text{IMI}}(R)$. Note that the equilibrium

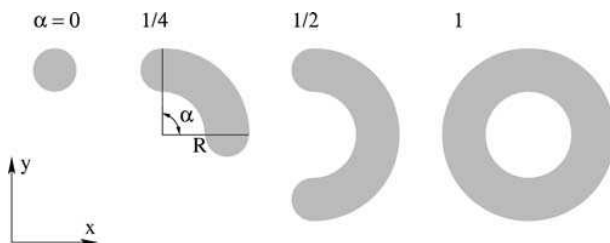


FIGURE 3 Parameterization of the elongated stalk. The shading schematically shows location of the hydrophobic segments in the plane of symmetry between fusing bilayers. The arc radius R corresponds to the radial distance to the outer hydrophilic/hydrophobic interface in the plane of symmetry. Values of the fractional arc angle α , defined in the range $[0, \pi]$, are given at the top of each stalk configuration. Note that $\alpha = 0$ corresponds to the original stalk, whereas $\alpha = \pi$ corresponds to a family of structures reminiscent of the IMI (see also Fig. 4).

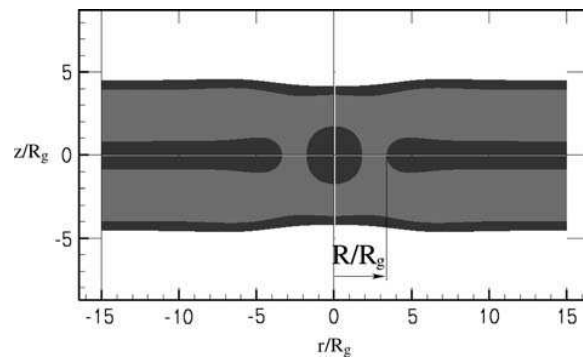


FIGURE 4 Density profile of an inverted micellar intermediate (IMI). The amphiphiles are characterized by $f = 0.3$. The radius of the IMI, in units of the radius of gyration, R/R_g is 3.4. Grayscale as in Fig. 1. The tension is zero.

IMIs considered by Siegel correspond to structures with an optimal radius R^* , which minimizes $F_{\text{IMI}}(R)$.

In general, the elongated stalk will not form a complete IMI, that is, α will be less than unity, so we approximate the free energy of the extended stalk in this configuration as

$$F_1(R, \alpha) = \alpha F_{\text{IMI}}(R) + F_S. \quad (5)$$

The presence of the second term is due to the free energy of the end caps of the extended stalk (see Fig. 3). As these two ends together form an axially symmetric stalk, the free energy of these ends is just the free energy of the classical stalk, F_S , which we have calculated previously (24). Note that for the case $\alpha = \pi$, the above estimate is certainly an upper bound as the second term should be absent in that case.

The free energy of the IMI can be calculated readily because it possesses the same axial symmetry as the stalk structure. The constraint on the position of the outermost A/B interface in the $z = 0$ symmetry plane is placed at a radius R (see Fig. 4). (For details, we refer the reader to Appendix A of Katsov et al. (24).) In Fig. 5 *a*, we show its free energy as a function of radius for a bilayer under zero tension for various architectural parameters f . Again, as is the case with the other axially symmetric structures we studied, the free energy is asymptotically linear at large R , with the slope $2\pi\lambda_{\text{IMI}}$ defining the effective line tension λ_{IMI} (see Eq. 4). In Fig. 5 *b* we also show the free energy of the IMI as a function of R for a bilayer with fixed $f = 0.31$ and different tensions. From Fig. 5 it is apparent that the free energy of the structure for the sizes that are pertinent to the fusion intermediate cannot be described by a simple estimate based on the line tension of the IMI. The increase of the free energy with decreasing radius at small radius results from the repulsion of the interfaces across the IMI structure. It is similar to the free energy barrier associated with closing the fusion pore (24). Note that the free energy does not decrease with R for large R because the IMI does not eliminate bilayer area. Therefore for large enough α and/or radius R , the free energy of this structure will exceed that of the stalk-hole complex in which

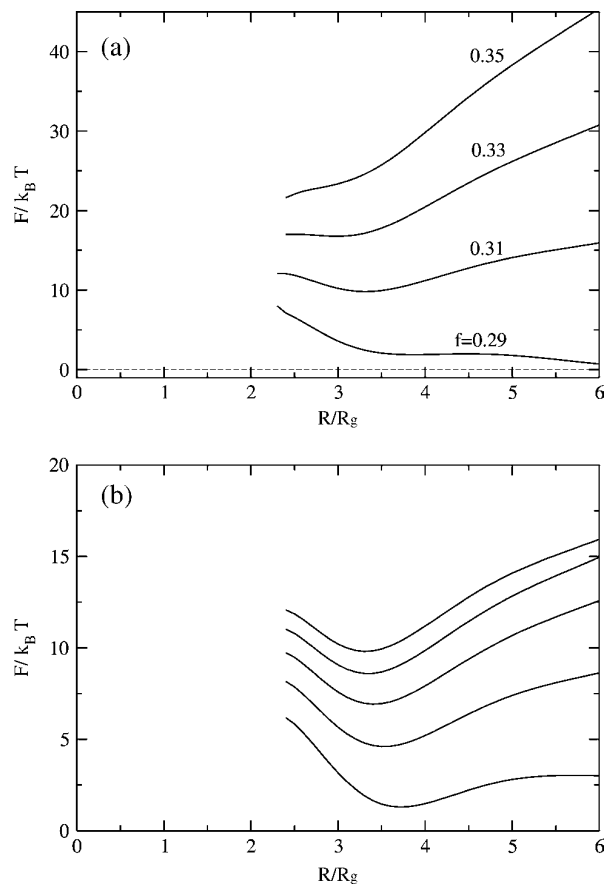


FIGURE 5 (a) Free energy of an IMI as a function of R/R_g at zero tension for various amphiphile architectures, f . (b) Free energy of an IMI with $f=0.31$ and for various tensions γ/γ_0 . From top to bottom, γ/γ_0 varies from 0.0 to 0.4 in increments of 0.1. The minima on these curves correspond to metastable IMI structures.

a hole forms next to the elongated stalk. We turn now to the calculation of the free energy of this complex.

Immediately after formation of stalk-hole complex

We model the stalk-hole complex as an elongated stalk in contact with a circular hole in one of the bilayers. We assume that the radial axes of the elongated stalk and of the hole coincide, and that the radius of the hole is $R - \delta$, where R is the radius of the elongated stalk, and that δ is chosen such that the hole is aligned in the radial direction with the elongated stalk over a fraction of its circumference, again denoted by α (see Fig. 6). To calculate the free energy of this configuration, we note that at $\alpha = 1$, the configuration is simply a hemifusion intermediate (HI) of radius R , and the elongated stalk would now connect two bilayers to one bilayer. We have calculated the free energy of the hemifusion intermediate previously (24). The radius R of this structure is defined by the position of the hydrophilic/hydrophobic inter-

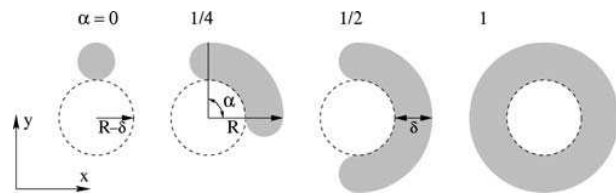


FIGURE 6 Parameterization of the stalk-hole complex. The shading schematically shows location of the hydrophobic segments in the plane of symmetry between fusing bilayers. The arc radius R corresponds to the radial distance to the hydrophilic/hydrophobic interface of the hemifusion intermediate in the plane of symmetry. Projection of the edge of a hole in one of the membranes is shown with dashed line. The radius of this hole is $R - \delta$. The other membrane does not have a hole. The hydrophobic thickness of the bilayer is δ . Values of the fractional arc angle α , defined in the range $[0, 1]$, are given at the top of each stalk configuration.

face in the $z = 0$ symmetry plane. With these definitions of the radii of the hemifusion intermediate and of the hole, a choice of $\delta(\gamma, f)$ equal to the hydrophobic thickness of a bilayer, ensures that the hole is adjacent to the elongated stalk. In general, when the hole forms, the elongated stalk does not completely surround it, so that a fraction $1 - \alpha$ of the stalk-hole complex looks like a bare hole edge in an isolated bilayer. Thus we approximate the free energy of this stalk-hole complex to be

$$F_2(R, \alpha) = \alpha F_{\text{HI}}(R) + (1 - \alpha) F_{\text{H}}(R - \delta) + F_d. \quad (6)$$

The free energy F_d comes from the end caps of the elongated stalk connecting to the hole edge. The two ends together do not make an axially symmetric stalk, but like the stalk, this defect is also saddle-shaped, so one expects its free energy to be small and not very different from that of the stalk.

The transition state

It is clear from Eqs. 5 and 6 that the free energies of these structures depend both on the radius, R , of the intermediate and on the fraction, α . Thus we must consider a two-dimensional reaction coordinate space, (R, α) . The fusion process starts off by the formation of the classical stalk, which corresponds to the $\alpha = 0$ line on the $F_1(R, \alpha)$ free energy surface. Elongation of the stalk corresponds to non-zero values of α . We assume that the stalk-hole complex forms when the free energy surfaces $F_1(R, \alpha)$ and $F_2(R, \alpha)$ intersect. This intersection happens along a line in the (R, α) plane, which defines the ridge of possible transition states $(R, \alpha_{\text{TS}}(R))$ with

$$\alpha_{\text{TS}}(R) = \frac{F_{\text{H}}(R - \delta) + F_d - F_s}{F_{\text{H}}(R - \delta) + F_{\text{IMI}}(R) - F_{\text{HI}}(R)}, \quad (7)$$

$$= 1 - \frac{F_{\text{IMI}}(R) - F_{\text{HI}}(R) + F_s - F_d}{F_{\text{H}}(R - \delta) + F_{\text{IMI}}(R) - F_{\text{HI}}(R)}. \quad (8)$$

The free energy of the optimal transition state can be obtained by finding the free energy minimum along the ridge of the

transition states, which we shall do momentarily. First we note from Eq. 8 that the fraction of the hole surrounded by the elongated stalk increases as the free energy of an isolated hole increases. This shows that the reduction of the high cost of the bare hole edge is a driving force of this mechanism.

We return to the free energy landscape of the fusion process defined by $\min(F_1(R, \alpha), F_2(R, \alpha))$. Examples of such landscapes are shown in Fig. 7. To clarify the effect of different parameters we present results for a membrane consisting of lipids with $f = 0.31$ and 0.33 , and under the reduced membrane tension $\gamma/\gamma_0 = 0.1$ and 0.2 . To obtain these results we have set the small defect energy F_d to zero. This parameter has very little effect on the qualitative features of the landscapes. Quantitative effects are also small and will be discussed below.

The landscapes are saddle-shaped, with low free energy valleys close to $\alpha = 0$ and $\alpha = 1$ lines. The first valley corresponds to barely elongated stalks of very small circumference, configurations which are clearly energetically inexpensive. The second valley corresponds to a hole that is almost completely surrounded by the elongated stalk. Its energy is small because formation of the hole leads to a decrease of the membrane area under tension. One should note that $\alpha = 1$ corresponds to the hemifusion intermediate, which is also formed in the standard mechanism, but through a completely different pathway.

The ridge of the transition states ($R, \alpha_{TS}(R)$) is indicated by a dotted line. There is a saddle point along this ridge, denoted by a circle on the plots. We denote the value of the

radius of this optimal transition state as R^* , and the value of $\alpha_{TS}(R^*)$ as α^* . The free energy of the transition state F^* is defined by $F^* \equiv F_1(R^*, \alpha^*) = F_2(R^*, \alpha^*)$. This assumes that one can ignore any additional barriers caused by the rearrangement of amphiphiles in passing from the configuration just before the formation of the stalk-hole complex, (i.e., the elongated stalk), to the configuration just after.

The value of α at the saddle point, α^* , is shown in Fig. 8. Once the stalk-hole complex has formed, the free energy of the complex decreases as the stalk continues to enclose the hole, that is, as α increases to unity. This is clear a priori because as the stalk advances around the perimeter of the hole, it reduces the large line tension of the bare hole to the smaller line tension of the hole surrounded by stalk without any concomitant increase in energy due to that advance.

For small values of the architectural parameter f , there is a considerable region for which $\alpha^* = 1$. The reason for this can be inferred from Fig. 9, which shows the calculated asymptotic (large R) values of the line tension, λ_{ES} , of the elongated stalk. One sees that λ_{ES} decreases as a function of f so that the free energy of an IML, $F_{IM}(R)$, which is dominated by this line tension, also decreases. Thus when the hole appears next to the extended stalk in a membrane characterized by a small f , more of the hole will be surrounded by the stalk, that is, α will increase toward unity. This physical explanation is reflected in Eq. 8.

We expect that this result has consequences for the amount of transient leakage during the fusion event. It is reasonable to expect that the amount of leakage would decrease as

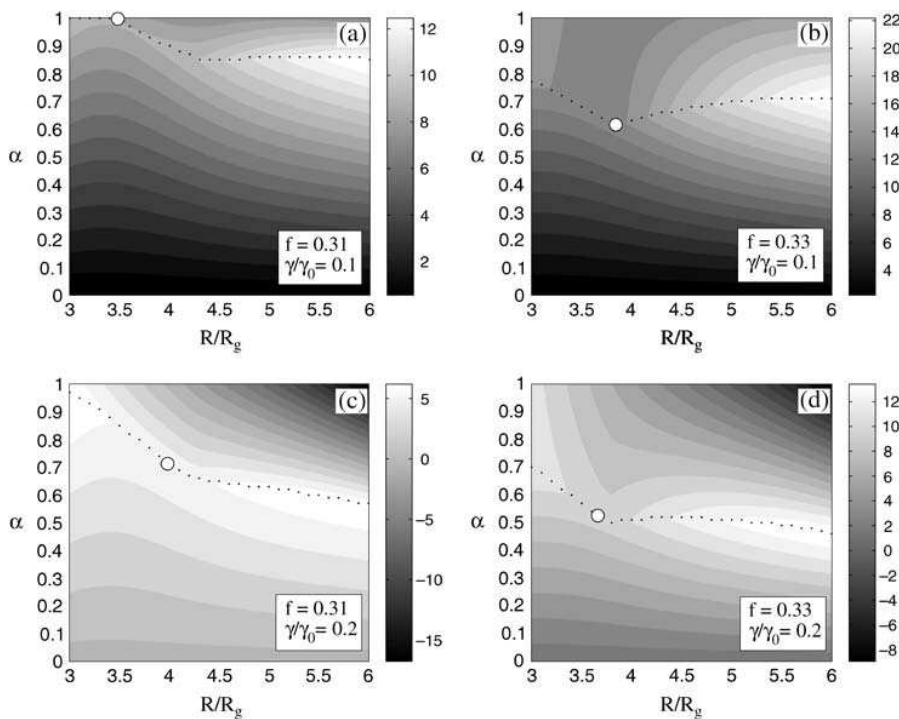


FIGURE 7 Four free energy landscapes (in units of $k_B T$) of the fusion process, plotted as a function of the radius, R (in units of R_g) and circumference fraction α . The architecture of the amphiphiles and the value of the tension γ/γ_0 are given. The dotted line shows a ridge of possible transition states, separating two valleys. The region close to the $\alpha = 0$ line corresponds to a barely elongated stalk intermediate (see Eq. 5). The other valley, close to $\alpha = 1$ states, corresponds to a hole almost completely surrounded by an elongated stalk. The saddle point on the ridge, denoted by an open dot, corresponds to the optimal (lowest free energy) transition state. The energy of the defect, F_d has been set to zero here.

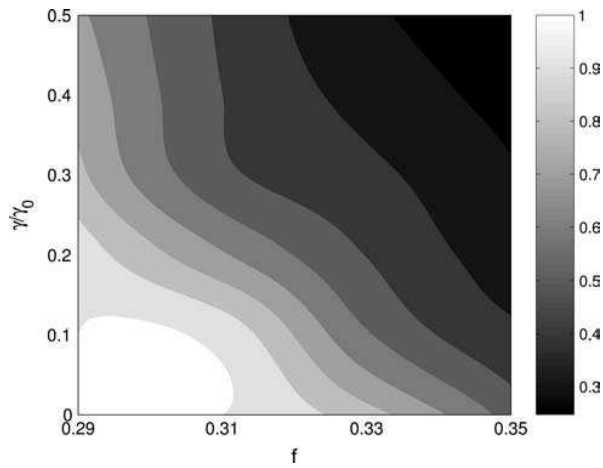


FIGURE 8 Plot of α^* , which corresponds to the optimal transition state in the stalk-hole mechanism, as a function of architecture of the amphiphiles and the tension of the membrane.

$(1 - \alpha)$, because this is the fraction of the hole in the stalk-hole complex which is not sealed by the stalk. In fact, for architectures with sufficiently small f (i.e., sufficiently large, negative spontaneous curvatures), Fig. 8 leads us to expect that $(1 - \alpha) = 0$, so that there would be no transient leakage at all.

The free energy barrier to formation of the stalk-hole complex measured relative to the initial metastable stalk, $(F^* - F_S)/k_B T$, is shown in Fig. 10 *a*. For comparison, we also show the barrier encountered in the standard hemifusion expansion mechanism, which we calculated earlier for the same parameters. It is clear that, in both mechanisms, the free energy barrier can be significantly lowered either by an increase in the membrane tension or decrease in the hydrophilic fraction f (more negative spontaneous curvature). The difference between these two barrier heights, in units of

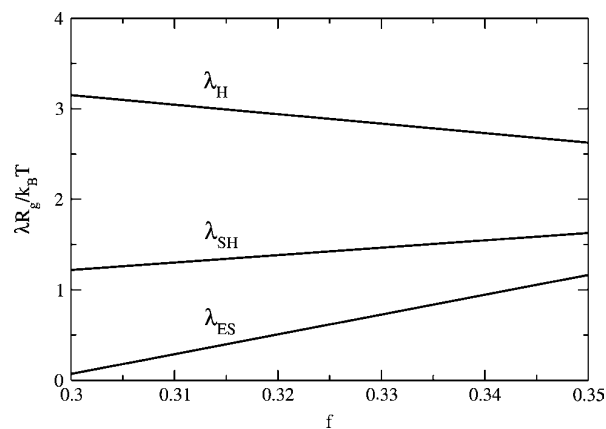


FIGURE 9 Line tensions of an elongated linear stalk, λ_{ES} , of a bare hole in a membrane, λ_H , and of a hole that forms next to an elongated stalk, λ_{SH} as a function of architecture, f . All line tensions are in units of $k_B T/R_g$.

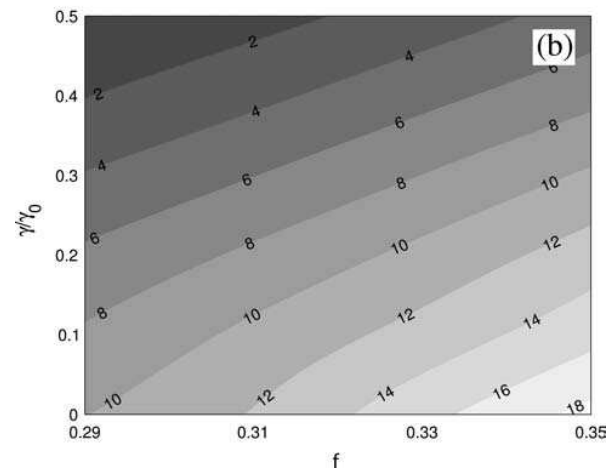
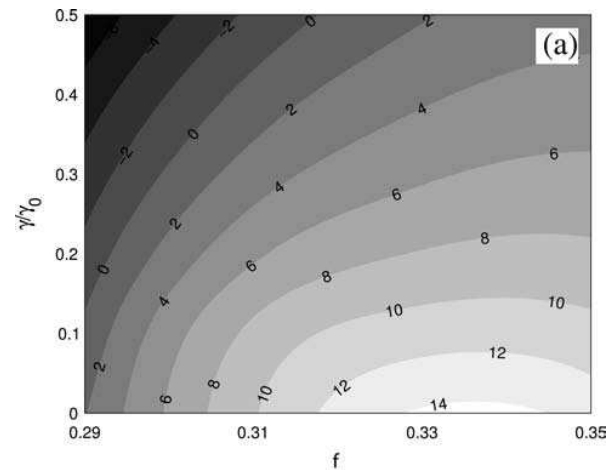


FIGURE 10 Free energy barriers measured relative to the initial metastable stalk, in units of $k_B T$, in (a) the new stalk-hole complex mechanism, and (b) the standard hemifusion mechanism.

$k_B T$, is shown in Fig. 11. It is positive when the barrier in the old mechanism exceeds that of the new mechanism. We see that over the entire region, the barrier to fusion is lower in the new mechanism, and becomes increasingly favorable as f decreases, i.e., as the amphiphile architecture becomes more inverted-hexagonal-forming. We estimate that the difference in barrier heights in this system of block copolymers, from ~ 1 to $7 k_B T$, would translate to a range of 3–18 $k_B T$ in a system of biological lipids.

As noted earlier, we have set the defect free energy, F_d , to zero in the above. Recall that the defect is the free energy of the two caps at the ends of the rim of an incomplete hemifusion diaphragm. As these caps are similar, but not identical, to the two halves of a stalk, we expect their energies to be similar. From our calculations (24), we know that the stalk free energy in our system does not exceed $4 k_B T$. If we set F_d to $4 k_B T$, then the difference in barrier heights in the two mechanism changes somewhat, and is shown in Fig. 11 *b*. The new mechanism is still favored over

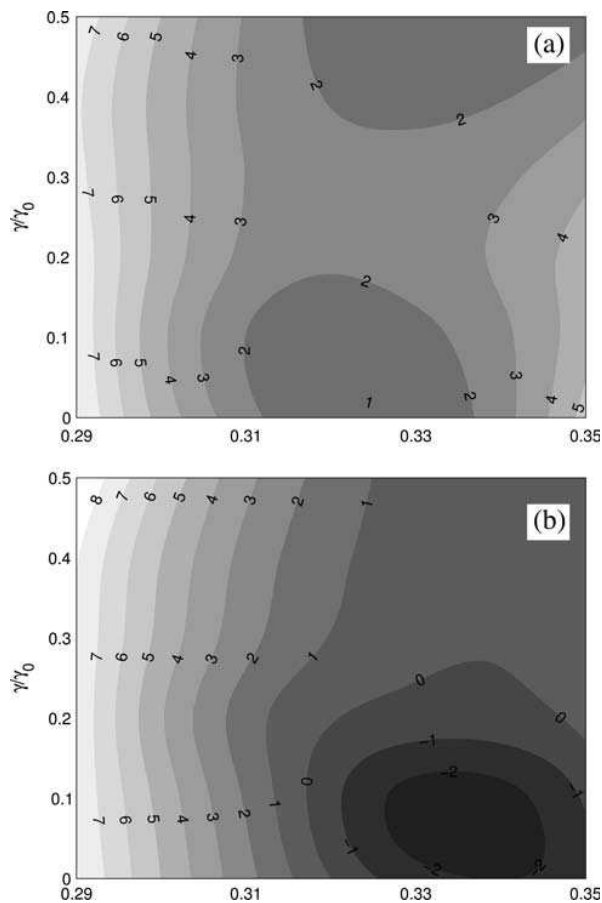


FIGURE 11 (a) Difference between the free energy barrier in the standard mechanism and that in the new mechanism, in units of $k_B T$, as a function of architecture, f_0 , and tension. The defect free energy is here taken to be zero. (b) Same as in a, except that the defect free energy is taken to be $4 k_B T$.

most of the tension/architecture space, and the standard mechanism is now favored for bilayers composed of amphiphiles with larger values of f , i.e., lamellar-forming lipids and under small tensions.

Formation of the final state

The stalk-hole complex is a transition state along the fusion pathway, but for complete fusion to occur it has to transform into a fusion pore. Properties of the fusion pore have been considered in detail in our first article (24). In the case of the standard hemifusion mechanism we have found that, for non-zero tensions, the fusion pore has a lower free energy than the hemifused transition state. Therefore, if the tension is maintained, the pore can presumably be formed without an appreciable additional barrier. In the present case, we have also found that the fusion pore has a lower free energy than the transition state, provided that the tension is not too small. We conclude, therefore, that formation of the stalk-hole complex involves the largest free energy barrier along this

pathway and pore formation should follow, provided the tension is maintained throughout the whole process. In a small region of low tension and small f , shown in black in Fig. 12, the stalk-hole transition state, which here is characterized by $\alpha = 1$, i.e., a completely formed IMI-like structure as in Fig. 4, has a lower free energy than a pore of the same radius. In this very special circumstance, the system may not continue on to the formation of a pore, but can remain in a metastable state in which the membranes are joined by an IMI structure.

DISCUSSION

We have utilized self-consistent field theory and a model of polymeric bilayers to calculate the free energy barriers along the fusion pathway first seen by Noguchi and Takasu and by ourselves (10,11). There are at least two barriers associated with this path; a smaller one associated with the formation of the initial axially symmetric classical stalk, and a larger one associated with the formation of the stalk-hole complex. This path replaces the expensive step in the old mechanism, which is the radial expansion of the stalk into a hemifusion diaphragm, by the expensive step of elongating the stalk in a wormlike fashion and having a hole form next to it which creates the stalk-hole complex. There are several points that we wish to make.

First, by direct comparison of the calculated free energy barriers in the new mechanism and in the standard one, we have demonstrated that the free energy barriers are comparable. Hence this new pathway is a viable alternative to the standard mechanism. We have also demonstrated that the new mechanism tends to be the more favorable, the more the amphiphile architecture approaches that of inverted-hexagonal formers.

Second, as noted previously, the new mechanism predicts the possibility of transient leakage which is correlated in

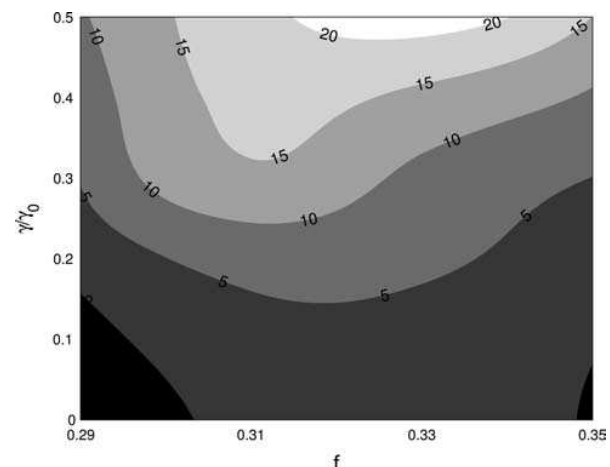


FIGURE 12 Difference in free energy, in units of $k_B T$, between the stalk-hole transition state and fusion pore of the same radius.

space and time with fusion. Just such leakage, correlated in space and time with fusion, has been observed (18). This prediction is in contrast with the old mechanism in which any leakage that occurs is not correlated directly with the fusion process itself. Our calculations predict that the amount of this correlated leakage decreases, and can vanish altogether, as the architecture of the amphiphiles becomes more like that of inverted-hexagonal formers. This is a prediction that could be tested by carrying out a series of experiments like those of Frolov et al. (18) on vesicles for which one could vary the amphiphile architecture or the relative composition of amphiphiles of different architecture. Such control of amphiphile architecture is readily obtained in polymersomes (39), which would therefore offer an excellent system in which to test this prediction.

Third, our calculations predict existence of metastable IMI-like structures, which have a free energy of formation higher than that of the fusion pore, except in a small region of very low f and γ where they are actually favored over a pore. Even in this region, the complete IMIs have a higher free energy than the unfused bilayers, and therefore are metastable. The possible occurrence of these structures had previously been dismissed due to very high estimates of the free energy of their formation (38).

Finally, we observe that, for this new mechanism to be favorable, two conditions must be met. The first is that it must not cost too much free energy for the stalk to elongate in a wormlike fashion, in the manner that it does before the hole appears. That this can be the case is clear from the fact that at the transition to an inverted hexagonal phase, the line tension of linear stalks is small. Thus as the architecture is varied such that the system approaches this transition, it must be inexpensive for the stalk to elongate and wander. That this is correct can be seen from the calculated line tension, λ_{ES} , of the elongated linear stalk shown in Fig. 9. It is essentially independent of tension, γ . We see that this line tension decreases with decreasing f as expected, which decreases the cost of elongating a stalk. The second condition is that the free energy of the hole which is created must not be too large. As noted earlier, the high cost of an isolated hole is due to the line tension of its periphery. If this is reduced by causing the hole to form next to the elongated stalk, the cost of the hole in the stalk-hole complex will also be reduced. To determine whether this is so, we have calculated the line tension of an isolated hole in a bilayer, λ_H , and also the line tension of a hole created next to an elongated stalk, λ_{SH} . These results, again essentially independent of the membrane tension, are shown in Fig. 9, as a function of architecture. It is seen that in the region of f in which successful fusion is possible, $0.29 < f < 0.37$ (24), the line tension of the hole is reduced by approximately a factor of 2. Let us now show that even such a relatively small change can have a very large effect on the rate of fusion.

Consider the simple estimate of the free energy of a hole, Eq. 4, which we reproduce here,

$$F_H = 2\pi\lambda_H R - \pi\gamma R^2. \quad (9)$$

The height of the barrier to stable hole formation corresponds to the maximum of this function. We ignore any R -dependence of λ_H and γ and immediately obtain the radius of the hole corresponding to the barrier to be $R^* = \lambda_H/\gamma$, and the height of the barrier to be $F^* = \pi\lambda_H^2/\gamma$. The rate of formation of an isolated hole in a bilayer is proportional to the Boltzmann factor

$$P_H = \exp\{-[F^* - k_B T \ln(A_H/\ell^2)]/k_B T\}, \quad (10)$$

$$= \frac{A_H}{\ell^2} \exp(-\pi\lambda_H^2/\gamma k_B T), \quad (11)$$

where the entropy associated with the formation of a hole in an available area A_H is $k_B \ln(A_H/\ell^2)$, with ℓ a characteristic length on the order of the bilayer width. If $P_H \ll 1$, then the bilayer is stable to hole formation by thermal excitation.

The formation of the stalk-hole complex reduces the line tension of that part of the hole near the stalk from λ_H to λ_{SH} . This can be described by introducing the effective average line tension entering Eq. 11,

$$\lambda_H \rightarrow \bar{\lambda}_\alpha \equiv \alpha\lambda_{SH} + (1 - \alpha)\lambda_H. \quad (12)$$

Then the corresponding rate of stalk-hole complex formation becomes

$$P_{SH} = \frac{N_S a_S}{\ell^2} \exp(-\pi\bar{\lambda}_\alpha^2/\gamma k_B T), \quad (13)$$

where N_S is the number of stalks formed in the system and a_S is the area around each stalk in which hole nucleation can take place. For the small reduction $\lambda_{SH}/\lambda_H = 1/2$, the above becomes

$$\frac{P_{SH}}{P_H} = \frac{N_S a_S}{A_H} \exp\left\{\frac{\pi\lambda_H^2}{\gamma k_B T} \left[\alpha \left(1 - \frac{\alpha}{4}\right)\right]\right\}, \quad (14)$$

$$= \frac{N_S a_S}{A_H} \left(\frac{A_H}{\ell^2 P_H}\right)^{\alpha(1-\alpha/4)}. \quad (15)$$

This shows explicitly that if the isolated membrane is stable to hole formation (i.e., $P_H \ll 1$), then even a small reduction in the line tension ensures that formation of the stalk/hole complex causes the rate of hole formation in the apposed bilayers, and therefore fusion, to increase greatly.

We illustrate this with two examples. We first consider the copolymer membranes that we simulated previously (9,10). In that case, the exponent in the Boltzmann factor is

$$-\frac{\pi\lambda_H^2}{\gamma k_B T} = -\pi \left(\frac{\lambda_H R_g}{k_B T}\right)^2 \left(\frac{\gamma_0}{\gamma}\right) \left(\frac{k_B T}{\gamma_0 R_g^2}\right), \quad (16)$$

where γ_0 is the tension of an interface between bulk hydrophilic and hydrophobic homopolymer phases. The various factors in the simulated system are $\lambda_H R_g/k_B T = 2.6$ at $f = 0.35$ (see Fig. 9), and $\gamma_0/\gamma = 4/3$, $k_B T/\gamma_0 R_g^2 = 0.31$, and $A_H/\ell^2 = 39$ (9,11). Note that, in the simulations, multiple stalks have

occasionally been observed. From these factors we obtain $P_H \approx 6 \times 10^{-3}$, so that isolated bilayers should have been stable to hole formation, as was indeed the case. However, in the presence of a stalk, the Boltzmann factor will be increased according to Eq. 15. If we assume that the elongated stalk enclosed one-half of the perimeter of the hole when it appeared (i.e., $\alpha = 1/2$), and that $N_S a_S / A_H \sim 0.3$ (consistent with the simultaneous observation of multiple stalks in a small simulation cell (10)), we find that $P_{SH} / P_H \sim 14$, so that the rate of hole formation should have increased appreciably as observed in the simulations. Figs. 6 and 8 of our previous work (9) clearly show that the rate of hole formation does increase by an order of magnitude. This increase is expected to be more dramatic in biological membranes. In that case we estimate the exponent of the Boltzmann factor, $-\pi \lambda_H^2 / \gamma k_B T$, as follows. We take the line tension to be that measured in a stearyloleoylphosphatidylcholine and cholesterol bilayer, $\lambda_H \approx 2.6 \times 10^{-6}$ erg/cm (34,35). For the surface tension, we take an estimate of the energy released by the conformational change of four of perhaps six hemagglutinin trimers arranged around an area of radius 4 nm, each trimer giving out $\sim 60 k_B T$ (40). This yields an energy per unit area $\gamma \approx 20$ erg/cm². Thus $P_H = 1.7 \times 10^{-11}$ (A_H / ℓ^2), which indicates that even subject to this large, local, energy-per-unit area, the membrane is quite stable to hole formation for vesicles of any reasonable size. However, if we assume again that the line tension of the hole is reduced by a factor of 2 by being nucleated next to the elongated stalk, that the stalk extends halfway around the circumference of the hole, and that the density of stalks is such that $N_S a_S / A_H = 0.3$, then the rate of hole formation is increased by

$$\frac{P_{SH}}{P_H} = 0.3 \left(\frac{1}{1.7 \times 10^{-11}} \right)^{7/16} \sim 1 \times 10^4, \quad (17)$$

i.e., an increase of more than four orders of magnitude.

One should note the implications of this simple argument. Because the probability to form a stable hole depends exponentially on the square of the line tension, an isolated bilayer is guaranteed to be stable against hole formation for normal line tensions. However, it is precisely this same dependence that also ensures that the bilayer will be destabilized by hole formation due to any mechanism that even modestly reduces that line tension. From here, it is only a short step to successful fusion.

We acknowledge very useful conversations and correspondence with M. Kozlov and S. J. Marrink.

This work was supported by the National Science Foundation under grant No. 0140500 and 0503752. Additional support was provided by the Volkswagen Foundation.

REFERENCES

- Blumenthal, R., M. J. Clague, S. Durell, and R. Eppard. 2003. Membrane fusion. *Chem. Rev.* 103:53–69.
- Jahn, R., and H. Grubmüller. 2002. Membrane fusion. *Curr. Opin. Cell Biol.* 14:488–495.
- Lentz, B. R., V. Malinin, M. E. Haque, and K. Evans. 2000. Protein machines and lipid assemblies: current views of cell-membrane fusion. *Curr. Opin. Struct. Biol.* 10:607–615.
- Mayer, A. 2002. Membrane fusion in eukaryotic cells. *Annu. Rev. Cell Dev. Biol.* 18:289–315.
- Skehel, J., and D. Wiley. 2000. Receptor binding and membrane fusion in virus entry: the influenza hemagglutinin. *Annu. Rev. Biochem.* 69: 531–569.
- Tamm, L., J. Crane, and V. Kiessling. 2003. Membrane fusion: a structural perspective on the interplay of lipids and proteins. *Curr. Opin. Struct. Biol.* 13:453–466.
- Kozlov, M. M., and V. S. Markin. 1983. Possible mechanism of membrane fusion. *Biofizika.* 28:255–261.
- Chernomordik, L. V., and M. M. Kozlov. 2003. Protein-lipid interplay in fusion and fission of biological membranes. *Annu. Rev. Biochem.* 72:175–207.
- Müller, M., K. Katsov, and M. Schick. 2003. A new mechanism of model membrane fusion determined from Monte Carlo simulation. *Biophys. J.* 85:1611–1623.
- Noguchi, H., and M. Takasu. 2001. Fusion pathways of vesicles: a Brownian dynamics simulation. *J. Chem. Phys.* 115:9547–9551.
- Müller, M., K. Katsov, and M. Schick. 2002. New mechanism of membrane fusion. *J. Chem. Phys.* 116:2342–2345.
- Marrink, S. J., and A. E. Mark. 2003. The mechanism of vesicle fusion as revealed by molecular dynamics simulations. *J. Am. Chem. Soc.* 125:11144–11145.
- Stevens, M. J., J. Hoh, and T. Woolf. 2003. Insights into the molecular mechanism of membrane fusion from simulation: evidence for the association of splayed tails. *Phys. Rev. Lett.* 91:188102-1–188102-4.
- Niles, W., M. Peeples, and F. Cohen. 1990. Kinetics of virus-induced hemolysis measured for single erythrocytes. *Virology.* 174:593–598.
- Cevc, G., and H. Richardsen. 1999. Lipid vesicles and membrane fusion. *Adv. Drug Des. Deliv.* 38:207–232.
- Evans, K. O., and B. R. Lentz. 2002. Kinetics of lipid rearrangements during poly(ethylene glycol)-mediated fusion of highly curved unilamellar vesicles. *Biochemistry.* 41:1241–1249.
- Lentz, B. R., W. Talbot, J. Lee, and L.-X. Zheng. 1997. Transbilayer lipid redistribution accompanies poly(ethylene glycol) treatment of model membranes but is not induced by fusion. *Biochemistry.* 36:2076–2083.
- Frolov, V. A., A. Y. Dunina-Barkovskaya, A. V. Samsonov, and J. Zimmerberg. 2003. Membrane permeability changes at early stages of influenza hemagglutinin-mediated fusion. *Biophys. J.* 85:1725–1733.
- Smit, J. M., G. Li, P. Schoen, J. Corver, R. Bittman, K.-C. Lin, and J. Wilschut. 2002. Fusion of α -viruses with liposomes is a non-leaky process. *FEBS Lett.* 421:62–66.
- Spruce, A., A. Iwata, and W. Almers. 1991. The first milliseconds of the pore formed by a fusogenic viral envelope protein during membrane fusion. *Proc. Natl. Acad. Sci. USA.* 88:3623–3627.
- Tse, F., A. Iwata, and W. Almers. 1993. Membrane flux through the pore formed by a fusogenic viral envelope protein during cell fusion. *J. Cell Biol.* 121:543–552.
- Lu, X., F. Zhang, J. McNew, and Y.-K. Shin. 2005. Membrane fusion induced by neuronal snares transits through hemifusion. *J. Biol. Chem.* 280:30538–30541.
- Meers, P., S. Ali, R. Erukulla, and A. Janoff. 2000. Novel inner monolayer fusion assays reveal differential monolayer mixing associated with cation-dependent membrane fusion. *Biochim. Biophys. Acta.* 1467:227–243.
- Katsov, K., M. Müller, and M. Schick. 2004. Field theoretic study of bilayer membrane fusion: I. hemifusion mechanism. *Biophys. J.* 87: 3277–3290.

25. Kozlovsky, Y., L. V. Chernomordik, and M. M. Kozlov. 2002. Lipid intermediates in membrane fusion: formation, structure, and decay of hemifusion diaphragm. *Biophys. J.* 83:2634–2651.
26. Loison, C., M. Mareschal, and F. Schmid. 2004. Pores in bilayer membranes of amphiphilic molecules: coarse-grained molecular dynamics simulations compared with simple mesoscopic models. *J. Chem. Phys.* 121:1890–1900.
27. Tolpekina, T., W. den Otter, and W. Briels. 2004. Simulations of stable pores in membranes: system size dependence and line tension. *J. Chem. Phys.* 121:8014–8020.
28. Tieleman, D., H. Leontiadou, A. Mark, and S. Marrink. 2003. Simulation of pore formation in lipid bilayers by mechanical stress and electric fields. *J. Am. Chem. Soc.* 125:6382–6383.
29. Leontiadou, H., A. Mark, and S. Marrink. 2004. Molecular dynamics simulations of hydrophilic pores in lipid bilayers. *Biophys. J.* 86:2156–2164.
30. Groot, R., and K. Rabone. 2001. Mesoscopic simulation of cell membrane damage, morphology change and rupture by nonionic surfactants. *Biophys. J.* 81:725–736.
31. Matsen, M. W. 1997. Thin films of block copolymer. *J. Chem. Phys.* 106:7781–7791.
32. Netz, R., D. Andelman, and M. Schick. 1997. Interfaces of modulated phases. *Phys. Rev. Lett.* 79:1058–1061.
33. Kasson, P., and V. S. Pande. 2004. Molecular dynamics simulation of lipid reorientation at bilayer edges. *Biophys. J.* 86:3744–3749.
34. Moroz, J. D., and P. Nelson. 1997. Dynamically stabilized pores in bilayer membranes. *Biophys. J.* 72:2211–2216.
35. Zhelev, D., and D. Needham. 1993. Tension-stabilized pores in giant vesicles—determination of pore size and pore line tension. *Biochim. Biophys. Acta.* 1147:89–104.
36. Rand, R. P., N. L. Fuller, S. M. Gruner, and V. A. Parsegian. 1990. Membrane curvature, lipid segregation, and structural transitions for phospholipids under dual-solvent stress. *Biochemistry.* 29: 76–87.
37. Flint, S., V. Racaniello, L. Enquist, A. Skalka, and R. Krug. 2000. *Virology: Molecular Biology, Pathogenesis, and Control.* ASM Press, Washington, DC. 136.
38. Siegel, D. P. 1993. Energetics of intermediates in membrane fusion: comparison of stalk and inverted micellar intermediate mechanisms. *Biophys. J.* 65:2124–2140.
39. Discher, B. D., Y.-Y. Won, D. S. Ege, J. C.-M. Lee, F. S. Bates, D. E. Discher, and D. A. Hammer. 1999. Polymersomes: tough vesicles made from diblock copolymers. *Science.* 284:1143–1146.
40. Kozlov, M., and L. Chernomordik. 1998. A mechanism of protein-mediated fusion: coupling between refolding of the influenza hemagglutinin and lipid rearrangements. *Biophys. J.* 75:1384–1396.